Hindawi
Geofluids
Volume 2021, Article ID 9374127, 10 pages
https://doi.org/10.1155/2021/9374127

Research Article

Control of Water Inrush from Longwall Floor Aquifers Using a Division Paste Backfilling Method

Qingliang Chang, Xingjie Yao, Shiguo Ge, Ying Xu, and Yuantian Sun

School of Mines, Key Laboratory of Deep Coal Resource Mining of the Ministry of Education, China University of Mining and Technology, Xuzhou, Jiangsu 221116, China

Correspondence should be addressed to Shiguo Ge; ts20020015a31@cumt.edu.cn and Ying Xu; kdxuying@163.com

Received 22 September 2021; Revised 24 October 2021; Accepted 1 November 2021; Published 25 November 2021

Academic Editor: Bailu Teng

Aiming at the problem of the safety mining problems of longwall paste filling working face under buildings on high confined water in the Daizhuang Coal Mine, the paste filling mining method was used. A series of theoretical analyses, numerical simulations, and field measurements were applied. The results showed that when the filling interval of the working face increases from 1.2 m to 3.6 m, no significant change is found in the depth of the perforated plastic zone of the floor strata. According to the types of water-conducting cracks in the floor strata of the working face 11607, the floor strata are divided into the floor intact area, the structure developed area, and the floor weak area. Based on that, the measures for preventing and controlling the floor failure in the paste filling working face are proposed. Furthermore, the failure depth of the floor of the test working face was detected by the on-site water injection method, and the results showed that the maximum failure depth of the floor of the test working face was about 3 m.

1. Introduction

Researchers in many countries have conducted a lot of theoretical research and practical applications on the prevention and treatment of coal mining under confined water by the backfill mining method [1–6]. To study and analyze the destruction depth and law of the underlying coal and rock during the mining process of the working face, water inrush from the underlying aquifer was studied by numerical modeling. The most dangerous position is in the section where the working face passes through the fault zone [7–10]. The underlying coal and rock layers were regarded as brittle rock masses, and the underlying water-conducting and nonconducting fracture surfaces were constructed. The probability of fracture and water inrush of the underlying coal seam increases with the increase of coal mining depth. The water inrush from the floor is directly related to the pressure of the mine [11–16].

Three-dimensional in situ stress was measured on-site, and according to the Mohr-Coulomb criterion, the results were obtained through FLAC3D numerical simulation analysis, to study and analyze the failure depth [17–20]. The plastic failure zone and stress field distribution law of the underlying coal strata at different coal mining stages are investigated. The on-site geophysical prospecting and drilling were used to study the damage depth of the underlying coal and rock during the mining process of coal seam faces in North China [21–23]. By detecting the displacement, deformation, and failure characteristics and stress field distribution of the underlying coal and rock layers before and after coal mining in the working face, the depth of deformation and failure of rock layers are obtained [24–26].

Aiming at the safe mining of the No. 16 coal seam in Daizhuang Coal Mine under buildings and high confined water conditions, the paste is used to fill the goaf area so that the filling body and the top and bottom of the goaf form a supporting system of the top plate-filling body-bottom plate. This technology can control the depth of the bottom plate damage and can play a better role in groundwater resources [27–30]. The protective effect of the coal mine, especially under the condition of coal mining under confined water, can significantly improve the safe production conditions of coal mines [31–34]. Furthermore, this technology can effectively control the surface subsidence and

deformation to achieve nonrelocation of coal mining, which can greatly improve coal resources. Also, the use of mine solid waste as a filling material can greatly improve the ecological environment of the mining area.

2. Project Overview

Daizhuang Coal Mine is located in Jining City, Shandong Province (Figure 1). It belongs to the conditions of coal mining under typical buildings and close-distance high-pressure water. There are 78 surface villages in the minefield. The mine is divided into the upper group of coal at the -410 m level and the lower group of coal at the -580 m level. The -410 m level mainly mines 3 upper and 3 lower coal seams, and the -580 m level mainly mines 16 and 17 coal seams.

According to the geological and hydrological drilling of the mine (Figure 2), it is proved that the distance between the No. 16 coal seam and the floor is 21.6 m on average, and the average distance from the Ordovician ash of the floor is 61.1 m. The positional relationship between the coal seam and the aquifer is shown in Figure 2. The maximum water inrush coefficient of the Ordovician ash aquifer in the No. 16 coal seam floor is about 0.12 MPa/m. The floor elevation of the working face is between -443.5 m and -516.9 m, and the average elevation is -501.3 m. The buried depth of the working face is between 480.6 and 558.3 m, with an average buried depth of 541.6 m. The thickness of the No. 16 coal seam in the working face is between 1.65 m and 2.35 m.

3. Analysis of Floor Failure Mechanism in Paste Filling Mining

3.1. Theoretical Analysis of Equivalent Roadway. When the working face is not filled with mining, as the working face continues to advance, the roof will undergo initial breakage and periodic breakage, and the pressure of the mine will appear stronger and obvious. When using filling mining, because the goaf behind the working face is continuously filled with paste, the timely support effect on the roof and floor can be used to look at the equivalent roadway that is continuously advancing, as shown in Figure 3. Therefore, the destruction depth of the underlying coal strata in backfill mining can be theoretically calculated using the equivalent roadway theory. For the exploration of the equivalent of the paste-filled working face into a moving roadway (or short-wall working face), the key question is how to determine the space effect and time effect of the equivalent moving roadway.

3.2. Spatial Effect on Equivalent Roadway Width. The width of the equivalent roadway is not the working face control roof distance, but it should be the distance from the coal wall to the filling body at a certain position behind the working face. The filling body at this position should meet certain requirements in terms of strength. With the difference in the paste filling process, the width of the equivalent roadway will also change. Parameters such as the solidification speed of the filling body, the daily footage of the working face, the filling step, and the roof control distance all affect the equivalent roadway.

(1) Before the coal mining machine cuts the coal after the open cut in the working face, the impact of mining on the working face is only the open cut, and the previous analysis has analyzed the open cut as an equivalent moving roadway, and the width of the roadway is the open cut. The width of the cut eye is L cut

(2) When the coal cutting footage of the working face is 1 filling step, it is widened compared to the equivalent moving roadway. Before the filling body solidifies and condenses, the width of the equivalent roadway is L branch + L step (where L step is a filling step, and L branch is the length of the top beam of the support), as shown in Figure 4(a)

(3) As the working face continues to cut coal forward when the coal cutting footage of the working face reaches 2 filling steps, it continues to expand and widen relative to the equivalent moving roadway. The age of the first filling zone in this period is 1 d; then, the width of the equivalent roadway at this time is $(L_{\text{branch}} + L_{\text{step}}) \sim (L_{\text{branch}} + 2L_{\text{step}})$. According to the practice of field engineering application, to ensure the safety of the calculation of the destruction depth value of the underlying coal strata, the width of the equivalent roadway is the largest $(L_{\text{branch}} + 2L_{\text{step}})$, as shown in Figure 4(b)

(4) After the goaf is filled with paste material, as the filling body condenses and solidifies, its strength continues to increase, supporting the roof and floor of the goaf. When the strength of the filling body is sufficient to transmit the overlying rock layer's self-weight load, the filling body at this position is regarded as a bunch of equivalents. At this time, the width of the equivalent roadway is $L_{\text{branches}} + nL_{\text{steps}}$ (the number of days for the filling body to reach the hydraulic pressure resistance is n), as shown in Figure 4(c)

(5) The distance between the coal wall and the filling zone of the working face after mining is the width of the final equivalent roadway. At this time, the maximum equivalent roadway width of the paste filling working face is $L_{\text{cut}} + nL_{\text{steps}}$. The minimum width is the open-cut eye width L_{cut}. The equivalent roadway width of the paste-filled working face in different states is different. The width of the equivalent roadway is $L_{\text{branch}} + n \times L_{\text{steps}}$, and the floor damage depth is the largest at this time

3.3. Time Effect on Equivalent Roadway Action. According to the observation results of general roadway deformation, it takes 30-40 days for a stable deformation. After the goaf is filled, the strength of the filling body gradually increases. The filling body prevents the top plate from continuing to sink and transmits the top plate load to the bottom plate. The time is taken by the floor from "excavation-support, support-exposed, filled area-backfill support" which is the time equivalent to the action of the mine pressure on the roadway. The calculation formula is as follows:

Figure 1: The location of Daizhuang Coal Mine.

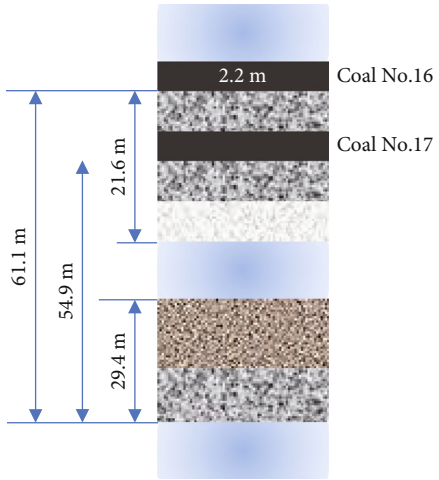

Figure 2: Location relationship between coal seam and aquifer.

$$T = \frac{L_{\text{branch}} + tL_{\text{step}}}{v}, \tag{1}$$

where L branch is the length of the support, m; T is the equivalent roadway action time, d; v is the advancing speed of the working face, m/d; and t is the time for the filling body to reach the water pressure resistance strength, d.

3.4. Bottom Failure Depth Analysis. Based on the equivalent roadway theory [35–38], the shape of the plastic failure zone of the working face floor with paste filling is shown in Figure 5. When the working face floor is damaged and the plastic failure range occurs, the plastic failure range of the working face floor is divided into the active limit range (such as area I in Figure 5), transition range (area II in Figure 5), and passive limit range (area III in Figure 5); the calculation formula of the floor failure depth can be derived from the theory of plastic slip line field:

$$h_{\text{po}} = \frac{l_a \cos\phi}{2\cos(\pi/4 + \phi/2)} \exp\left[\left(\frac{\pi}{4} + \frac{\phi}{2}\right)\tan\phi\right]. \tag{2}$$

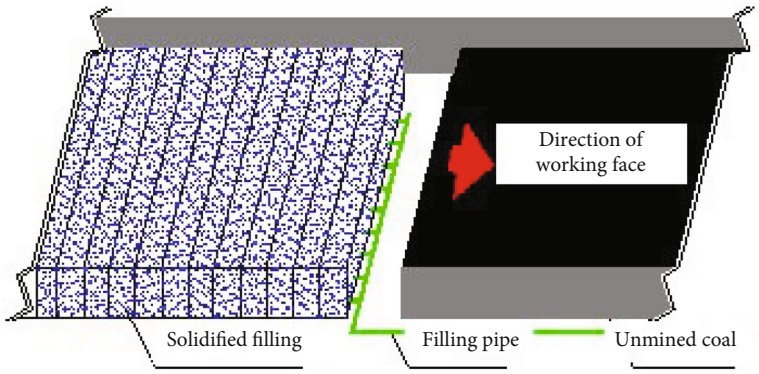

Figure 3: Schematic diagram of longwall paste filling working face.

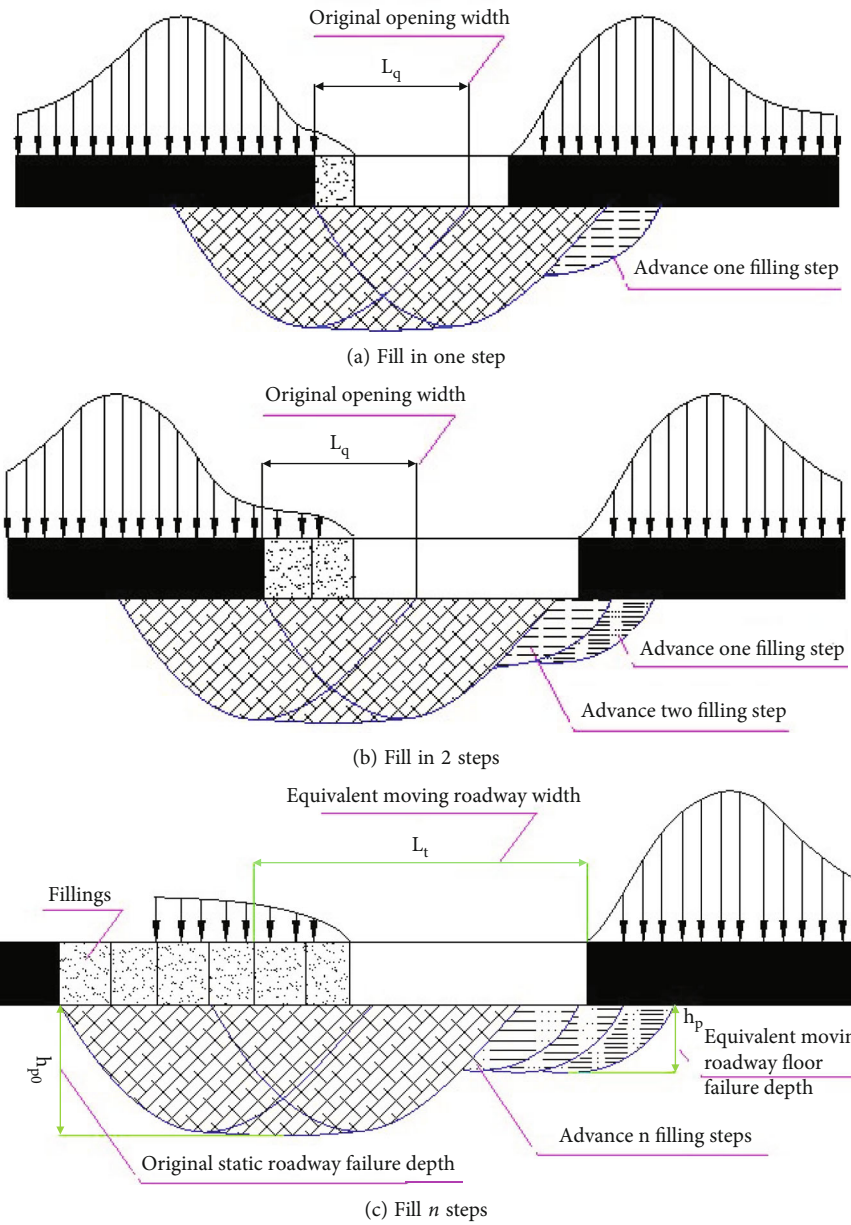

Figure 4: The relationship between equivalent roadway width and floor failure depth.

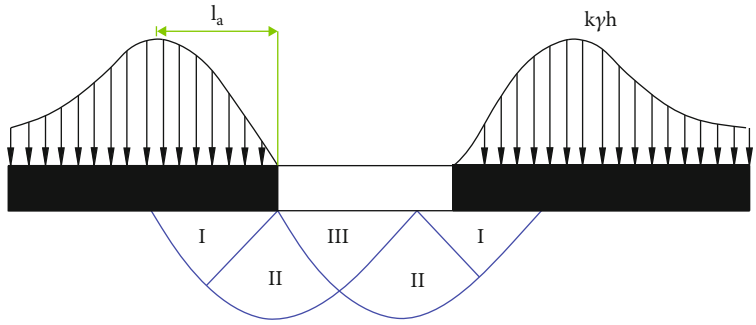

Figure 5: Calculation model of equivalent roadway floor failure depth.

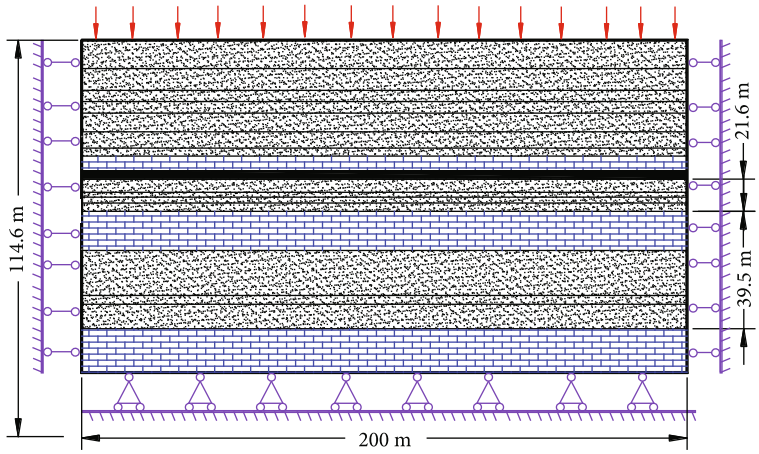

Figure 6: Numerical simulation models and boundary conditions.

In the formula, h_{po} is the depth of coal and rock failure under the paste filling face, m; l_a is the width of the plastic zone on the two sides of the roadway, m; and φ is the internal friction angle of the coal seam floor.

4. Numerical Simulation Analysis of Floor Failure

4.1. Model Construction and Program Design. The simulation uses FLAC numerical simulation software. Combining the comprehensive histogram of the 11607 working face on the Daizhuang Coal Mine site and the actual conditions of the four geological boreholes *L*10-2, *L*10-4, 11607-2, and 15-2 in the underlying coal seam, the numerical simulation is based on the lower part of the 11607 working face. The height and width of the constructed model are 114.6 m and 200 m, respectively. The cutting height of the 11607 working face is 2 m. The distance between the No. 16 coal seam and the uppermost boundary of the model is 39.6 m, and the distance from the bottom boundary of the model is 75 m. The upper bound of gray is 61.1 m away, and the distance from the upper thirteenth upper bound of the lower part is 21.6 m. The numerical simulation model is shown in Figure 6. In the design model, the inclined length of the 11607 paste filling working face is 120 m, and an open cut is arranged at the left end of the model 50 m, and the mining advances from the left end of the model to the right. The width between the left and right boundaries of the design model is 200 m. The rock mass parameters are given in Table 1.

This simulation is mainly aimed at the research and analysis of the relationship between the different filling process parameters of the paste filling working face and the floor failure depth under the conditions of different filling body strength, filling step, and filling rate at 11607 paste filling working face. First, the coal mining operation is carried out, the goaf is followed by the filling operation, and finally, the working face is overhauled. At the same time, the paste filling body is solidified, and the goaf is filled. The step distance is consistent with the daily footage of the working face, and the numerical simulation plan is designed according to the site conditions: (1) the simulation setting 11607 working face goaf is 98% filling rate, filling step 2.4 m/d, and simulation. The 28 d strength of the filling body is 3 MPa, 4 MPa, 5 MPa, and 7 MPa; (2) the strength (28 d strength) of the paste filling body in the goaf area of 11607 working faces is set to 5 MPa, and the filling rate is 98%. Then, the filling step distance distribution of the simulated paste filling body is 1.2 m, 2.4 m, and 3.6 m.

4.2. Analysis of the Results of Numerical Simulations. According to the simulation results of numerical simulation plan 1 and plan 2, under the conditions of different filling strength parameters, the simulation results of the failure depth of the

Table 1: The rock mass properties.

No.	Lithology	Density (kg/m^3)	Bulk modulus (GPa)	Shear modulus (GPa)	Cohesion (MPa)	Friction angle (°)	Tensile strength (MPa)
1	Grit stone	2450	31.37	23.51	8.61	44	9.12
2	Fine stone 11 sandstone	2600	19.71	14.62	6.52	37	6.94
3	Medium stone	2550	31.35	20.51	6.80	42	7.61
4	Siltstone	2650	16.35	12.24	4.69	31	2.36
6	Coal	1450	0.78	0.45	2.21	22	0.41
7	Mudstone	2250	7.11	3.98	3.45	35	0.89

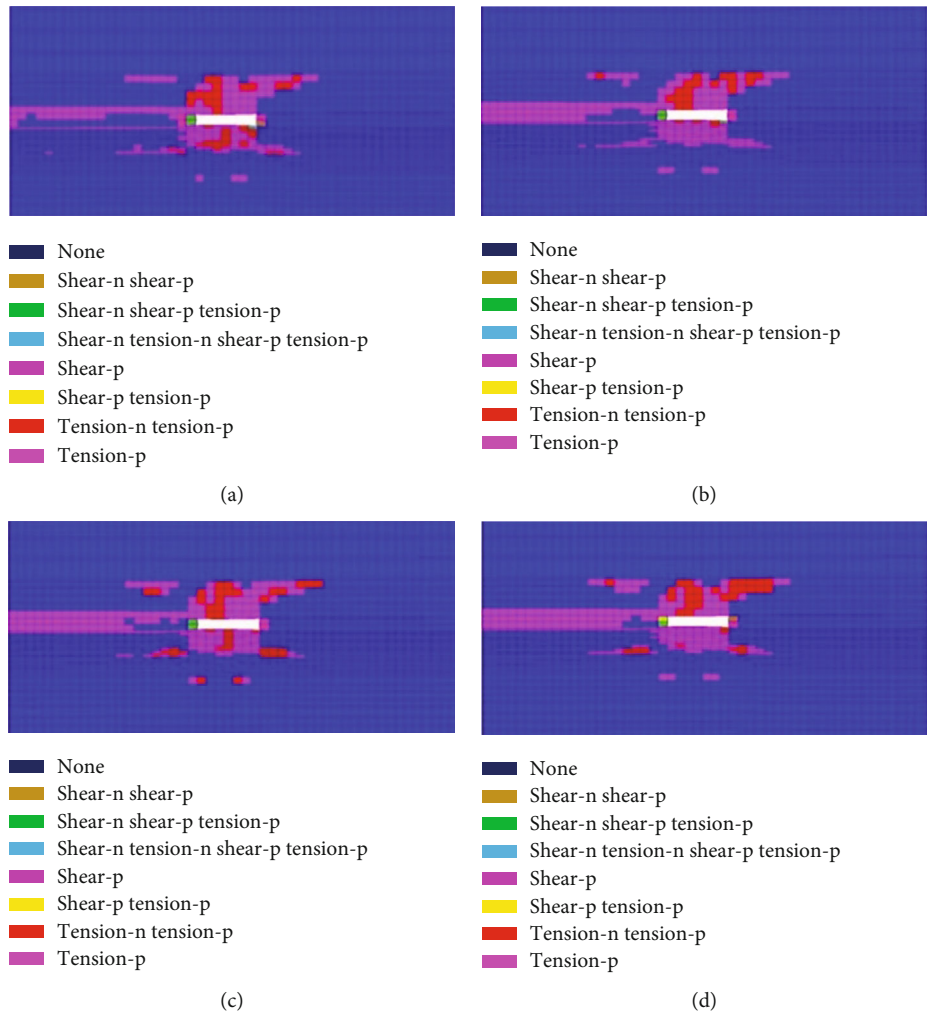

Figure 7: Numerical simulation of the plastic zone of 28 d strength of the different paste: (a) 3 MPa, (b) 4 MPa, (c) 5 MPa, and (d) 7 MPa.

floor of the paste filling working face, the deformation of the rock formation, and the distribution of the plastic zone are shown in Figures 7 and 8 (A section is taken at the middle of the advancing direction of the 11607 working face).

It can be seen from the analysis in Figure 7 that when the 28 d strength of the filling paste on the 11607 working face increases from 3 MPa to 7 MPa, the peak subsidence of the overlying coal strata on the working face also shows a downward trend, and the peak subsidence drops from 250 mm to 200 mm. The bottom heave of the working face has no obvious deformation. When the 28 d strength of the filling paste on the 11607 working face increased from 3 MPa to 7 MPa, no

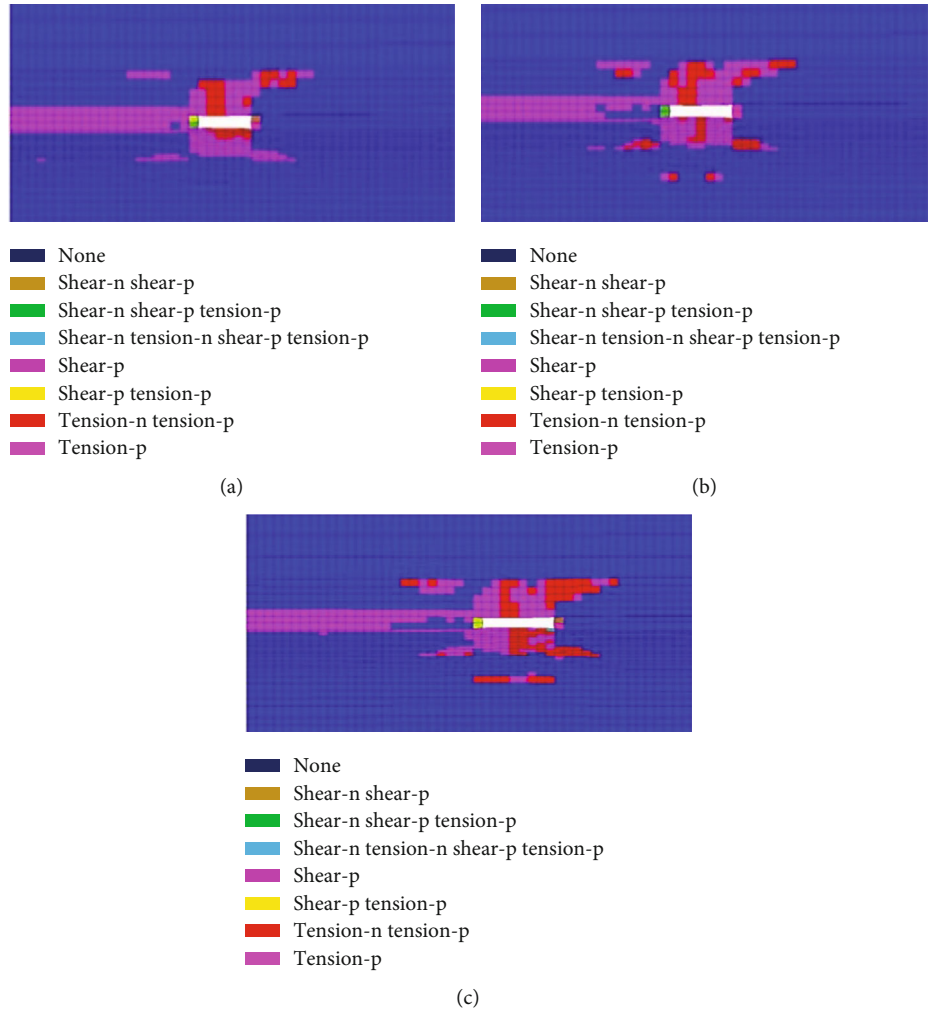

Figure 8: The plastic zone is numerically simulated with different filling steps: (a) 1.2 m, (b) 2.4 m, and (c) 3.6 m.

significant change was found in the depth of the penetrated plastic zone of the coal and rock layer beneath the working face, and only its range slightly decreased.

It can be seen from Figure 8 that when the filling step of the 11607 working face increases from 1.2 m to 3.6 m, the peak subsidence of the overlying coal strata on the working face also shows an upward trend, and the peak subsidence rises from 180 mm to 250 mm. Obvious deformation of the bottom drum of the working face occurs, and the peak value of the bottom drum rises from 180 mm to 200 mm. When the filling step of the 11607 working face was increased from 1.2 m to 3.6 m, no significant change was found in the depth of the penetrated plastic zone of the coal and rock layer beneath the working face. When the filling steps are 1.2 m, 2.4 m, and 3.6 m, the depth of the plastic zone penetrated by the coal strata beneath the working face is approximately 3.6 m, and the coal strata beneath the working face penetrate to the bottom mudstone and fine-grained sandstone. Floor. The plastic zone of the coal and rock layer beneath the working face presents a process from layered failure to final penetration. When the filling step is 2.4 m, the plastic zone in the lower coal layer of the working face extends to the siltstone layer at a distance of about 6.3 m; when the filling step is 3.6 m, the depth of the plastic zone in the lower coal layer of the working face is still at the lower distance The siltstone layer is about 6.3 m away, but the extent of the plastic zone tends to further increase.

Based on the above analysis, it can be concluded that after the open-cut hole is excavated in the paste filling face, as the face continues to advance coal mining, paste fill the mined area in the goaf behind the face, and the roof of the mined area is no longer. The initial collapse and periodic collapse occur, which is equivalent to the continuous advancement of the open cut in the coal mining process, and the open cut is a special roadway, so the paste filling face is equivalent to the mine pressure generated by the special roadway that is continuously advancing which has a low degree of disturbance to the stress field of the surrounding rock of the roof and floor. The appearance of the mine pressure is very similar to that of the excavation roadway. The difference lies in the maximum vertical stress and plasticity of the filling body in the goaf. The area is smaller than that near the coal wall, and the maximum vertical displacement near the backfill is larger than that near the coal wall. Based on the analysis of the numerical simulation results and the previous theoretical calculations, combined with the actual on-site mining of the 11607 paste filling face of Daizhuang

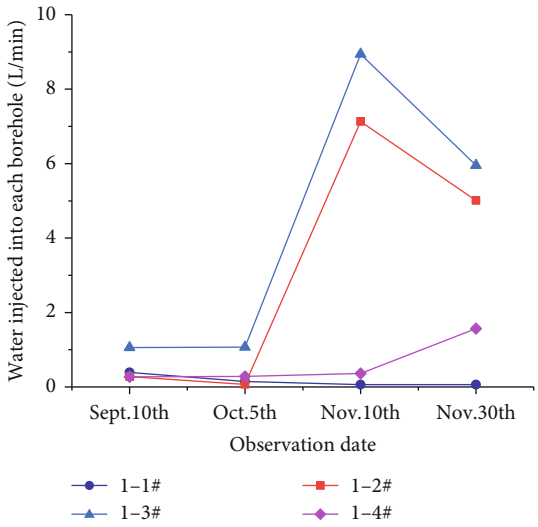

Figure 9: 1# water injection into each borehole at test point.

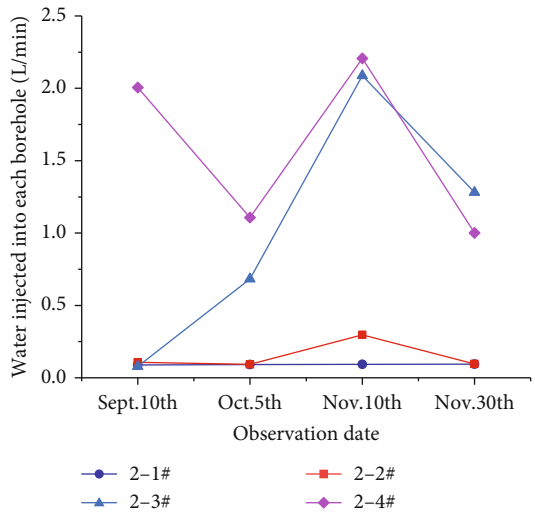

Figure 10: Water injection test results of 1# station.

Coal Mine, and referring to mining practical experience, it is theoretically estimated that the 11607 working face adopts the paste filling technology and then the underlying coal. The depth of rock failure is between 4.6 m and 8.4 m.

5. Field Engineering Application

5.1. Parameter Design. According to the geological report and on-site investigation of the 11607 working face of Daizhuang Coal Mine in the early stage, and according to the types of water-conducting cracks in the underlying coal and rock layers of the working face, the underlying coal and rock layers of the 11607 working face are roughly classified into the following three categories: (1) complete floor area, (2) tectonic development zone, and (3) weak floor zone. The technical measures and safety guarantee methods for the prevention and control of water inrush from the floor are proposed for different areas such as the complete block of the floor, abnormal hydrological detection or high pressure, and weak floor or structurally developed blocks:

(1) Only paste is used to fill the goaf in the complete area of the 11607 working face floor, and the floor is not treated. The design mass concentration of the paste material to fill the goaf is 78%, and the amount of coal gangue, fly ash, and cement is, respectively, 1600 kg/m^3, 400 kg/m^3, and 60 kg/m^3. (2) Weak floor area, combined with simulation and on-site paste filling working face mine pressure influence range, initially determines the weak area to be 50 m outward for floor grouting transformation. (3) The fault-affected area, combined with the simulation and the on-site paste-filling working face's underground pressure influence range, it is preliminarily determined that the F11605-2, F11605-3, and DF16 faults will be reinforced and plugged by floor grouting within 50 m outwards. For small faults exposed in the working face, it is necessary to consider the actual situation of on-site drilling and comprehensive analysis to consider whether to carry out floor grouting reinforcement and plugging reconstruction. (4) High water pressure areas and detection of hydrological abnormal areas, 11607 working face adopts paste filling. After the mined-out area technology, the impact range of the mine pressure around the stope is less than 50 m, so the preliminary design is carried out on the proven high water pressure area of the underlying coal and rock layer (water pressure greater than 4.4 MPa) and the area where hydrological anomalies have been detected at the working face. For dredging treatment, the dredging range is within 100 m from the left to the right and the front and back of the working face.

5.2. Field Application Effect Analysis. Through on-site investigation of the mining practice of Daizhuang Coal Mine 11607 working face, water injection tests were carried out in the track lane of 11607 working face to observe the destruction depth of the underlying coal and rock layers. It is selected to be carried out at a position 150 m away from the stop line of 11607 working face, and two detection points numbered 1# and 2# are arranged. The distance between the two detection points is about 15 m, and both detection points 1# and 2# are arranged 4 water injection test boreholes for observing the destruction depth of the underlying coal and rock layers, and the distance between the water injection test boreholes is 2 m. The elevation and depression angles of the water injection boreholes arranged in the 1# detection point and the No. 16 coal seam are both 60°, and the destruction depths of the underlying coal strata are observed to be 2 m, 3 m, 5 m, and 7 m in sequence. The water injection boreholes arranged in the 2# detection point are perpendicular to the No. 16 coal seam, and the destruction depth of the underlying coal strata is observed to be 2 m, 3 m, 5 m, and 7 m in order. The detection results are as follows:

The water injection volume change curve of each borehole at 1# detection point is shown in Figure 9. Through analysis, it can be seen that the water injection volume of the 1-2# borehole with a depth of 3 m and the 1-3# borehole with a depth of 5 m has relatively large changes. The fluctuation changes are more obvious, while the 1-1# drill hole with a depth of 2 m and the drill hole 1-4# with a depth of 7 m injected lower water volume, and the fluctuation change is not obvious,

indicating that the depth of the underlying coal strata at the working face is 3~ coal, and rock mass cracks within 5 m are more developed, and the depth is greater than that of the coal and rock mass underneath the working face. The degree of development of the cracks is relatively low. Based on the above analysis, the depth of the floor is less than 3~5 m after adopting the paste filling technology in the 11607 working face.

The water injection volume change curve of each borehole at the 2# detection point is shown in Figure 10. The analysis shows that the water injection volume of the four boreholes 2-1#, 2-2#, 2-3#, and 2-4# is relative to that of 1#. The boreholes at the detection points are relatively small, and the water injected into the 2-2# borehole with a depth of 2 m and the 2-4# borehole with a depth of 8 m is 0 L/min, indicating that the depth of the underlying coal strata at the working face is 2 m. The cracks in the coal and rock masses are relatively developed, and the depth is greater than that of the coal and rock masses under the working face. The degree of development of the cracks in the coal and rock masses underneath the working face is relatively low. The destruction depth is about 2 m.

6. Conclusion

(1) Based on the equivalent roadway theory, when the advancing speed of the working face is 1.2~3.6 m/d and the water pressure resistance of the filling body does not exceed 2 d, the failure depth of the floor of the paste filling working face is 4.6~8.4 m

(2) According to the geological report and field survey of the 11607 working face, the floor coal and rock layers of the 11607 working face are divided into three regions. According to the different zones of the floor, technical measures and safety guarantee methods for the prevention and control of water inrush from the floor are proposed

(3) Detect by using the water injection test method on-site, it is concluded that the maximum damage depth of the bottom plate is about 3 m

Data Availability

The Microsoft Excel Worksheet data used to support the findings of this study are available from the corresponding author upon request.

Conflicts of Interest

The authors declare that they have no competing interests.

Acknowledgments

This research was supported by the projects of "the Fundamental Research Funds for the Central Universities (2020ZDPY0221 and 2021QN1003)," "the National Natural Science Foundation of China (52174130, 52104106, and 52174089)," and the Basic Research Program of Xuzhou (KC21017).

References

[1] X. Shi, H. Zhou, X. Sun, Z. Cao, and Q. Zhao, "Floor damage mechanism with cemented paste backfill mining method," *Arabian Journal of Geosciences*, vol. 14, no. 2, pp. 1–9, 2021.

[2] Q. Sun, G. Meng, K. Sun, and J. Zhang, "Physical simulation experiment on prevention and control of water inrush disaster by backfilling mining under aquifer," *Environmental Earth Sciences*, vol. 79, no. 18, pp. 1–17, 2020.

[3] W. Sun, S. Zhang, W. Guo, and W. Liu, "Physical simulation of high-pressure water inrush through the floor of a deep mine," *Mine Water and the Environment*, vol. 36, no. 4, pp. 542–549, 2017.

[4] Y. Sun, G. Li, J. Zhang, J. Sun, and J. Xu, "Development of an ensemble intelligent model for assessing the strength of cemented paste backfill," *Advances in Civil Engineering*, vol. 2020, 6 pages, 2020.

[5] S. Yu, J. Xu, W. Zhu, S. Wang, and W. Liu, "Development of a combined mining technique to protect the underground workspace above confined aquifer from water inrush disaster," *Bulletin of Engineering Geology and the Environment*, vol. 79, no. 7, pp. 3649–3666, 2020.

[6] Q. Bai, S. Tu, C. Zhang, and D. Zhu, "Discrete element modeling of progressive failure in a wide coal roadway from water-rich roofs," *International Journal of Coal Geology*, vol. 167, pp. 215–229, 2016.

[7] J. Liu, G. Li, S. Yang, and J. Huang, "Prediction models for evaluating the strength of cemented paste backfill: a comparative study," *Minerals*, vol. 10, no. 11, p. 1041, 2020.

[8] H. Rong, G. Li, D. Liang, C. Sun, S. Zhang, and Y. Sun, "Numerical investigation on the evolution of mechanical properties of rock affected by micro-parameters," *Applied Sciences*, vol. 10, no. 14, p. 4957, 2020.

[9] Y. Sun, G. Li, J. Zhang, B. Yao, D. Qian, and J. Huang, "Numerical investigation on time-dependent deformation in roadway," *Advances in Civil Engineering*, vol. 2021, 7 pages, 2021.

[10] J. Zhao, J. Chen, X. Zhang, J. Ning, and Y. Zhang, "Distribution characteristics of floor pore water pressure based on similarity simulation experiments," *Bulletin of Engineering Geology and the Environment*, vol. 79, no. 9, pp. 4805–4816, 2020.

[11] Q. Bai and S. Tu, "A general review on longwall mining-induced fractures in near-face regions," *Geofluids*, vol. 2019, Article ID 3089292, 22 pages, 2019.

[12] C. Eriksson and A. Nyström, "Garpenberg mine–10 years of mining with paste backfill," in *Proceedings of the 21st International Seminar on Paste and Thickened Tailings*, pp. 323–336, Perth, Australia, 2018.

[13] G. Li, Z. Jiang, C. Lv, C. Huang, G. Chen, and M. Li, "Instability mechanism and control technology of soft rock roadway affected by mining and high confined water," *International Journal of Mining Science and Technology*, vol. 25, no. 4, pp. 573–580, 2015.

[14] W. Liu, D. Mu, X. Xie, L. Yang, and D. Wang, "Sensitivity analysis of the main factors controlling floor failure depth and a risk evaluation of floor water inrush for an inclined coal seam," *Mine Water and the Environment*, vol. 37, no. 3, pp. 636–648, 2018.

[15] K. Ma, X. Sun, C. Tang, F. Yuan, S. Wang, and T. Chen, "Floor water inrush analysis based on mechanical failure characters and microseismic monitoring," *Tunnelling and Underground Space Technology*, vol. 108, article 103698, 2021.

[16] W. Song, Z. Liang, and C. Zhao, "Mechanical failure characteristics of mining floor along working face inclination above confined water," *Chinese Journal of Rock Mechanics and Engineering*, vol. 37, no. 9, pp. 144–156, 2018.

[17] M.-K. Bo, "Analysis on reverse fault activation and water inrush possibility for coal mining above confined aquifer in a mining area," *Journal of China Coal Society*, vol. 36, no. 7, pp. 1177–1183, 2011.

[18] J. Chen, J. Zhao, S. Zhang, Y. Zhang, F. Yang, and M. Li, "An experimental and analytical research on the evolution of mining cracks in deep floor rock mass," *Pure and Applied Geophysics*, vol. 177, no. 11, pp. 5325–5348, 2020.

[19] J. Zhang, "Investigations of water inrushes from aquifers under coal seams," *International Journal of Rock Mechanics and Mining Sciences*, vol. 42, no. 3, pp. 350–360, 2005.

[20] S. Zhang, W. Guo, and Y. Li, "Experimental simulation of water-inrush disaster from the floor of mine and its mechanism investigation," *Arabian Journal of Geosciences*, vol. 10, no. 22, pp. 1–11, 2017.

[21] H. Gui, X. Song, and M. Lin, "Water-inrush mechanism research mining above karst confined aquifer and applications in north China coalmines," *Arabian Journal of Geosciences*, vol. 10, no. 7, p. 180, 2017.

[22] Y. Hu, W. Li, Q. Wang, S. Liu, and Z. Wang, "Evolution of floor water inrush from a structural fractured zone with confined water," *Mine Water and the Environment*, vol. 38, no. 2, pp. 252–260, 2019.

[23] Y. Sun, R. Bi, Q. Chang et al., "Stability analysis of roadway groups under multi-mining disturbances," *Applied Sciences*, vol. 11, no. 17, p. 7953, 2021.

[24] N. J. Koupouli, T. Belem, P. Rivard, and H. Effenguet, "Direct shear tests on cemented paste backfill-rock wall and cemented paste backfill-backfill interfaces," *Journal of Rock Mechanics and Geotechnical Engineering*, vol. 8, no. 4, pp. 472–479, 2016.

[25] Z. Liang, W. Song, and W. Liu, "Theoretical models for simulating the failure range and stability of inclined floor strata induced by mining and hydraulic pressure," *International Journal of Rock Mechanics and Mining Sciences*, vol. 132, article 104382, 2020.

[26] S. Liu, W. Liu, and J. Shen, "Stress evolution law and failure characteristics of mining floor rock mass above confined water," *KSCE Journal of Civil Engineering*, vol. 21, no. 7, pp. 2665–2672, 2017.

[27] M. He, P. Guo, J. Wang, and H. Wang, "Experimental study on gob-side entry formed by roof cut of broken roof at shallow depth of hecaogou no. 2 coalmine," *Chinese Journal of Geotechnical Engineering*, vol. 40, no. 3, pp. 391–397, 2018.

[28] W. Li, Y. Liu, W. Qiao, C. Zhao, D. Yang, and Q. Guo, "An improved vulnerability assessment model for floor water bursting from a confined aquifer based on the water inrush coefficient method," *Mine Water and the Environment*, vol. 37, no. 1, pp. 196–204, 2018.

[29] V. Odintsev and N. Miletenko, "Water inrush in mines as a consequence of spontaneous hydrofracture," *Journal of Mining Science*, vol. 51, no. 3, pp. 423–434, 2015.

[30] Y. Sun, G. Li, J. Zhang, J. Sun, J. Huang, and R. Taherdangkoo, "New insights of grouting in coal mass: from small-scale experiments to microstructures," *Sustainability*, vol. 13, no. 16, p. 9315, 2021.

[31] G. Li, Y. Sun, J. Zhang et al., "Experiment and application of coalcrete on roadway stability: a comparative analysis," *Advances in Materials Science and Engineering*, vol. 2020, 14 pages, 2020.

[32] M. Li, J. Zhang, W. Zhang, A. Li, and W. Yin, "Experimental investigation of water-inrush risk based on permeability evolution in coal mine and backfill prevention discussion," *Geofluids*, vol. 2019, Article ID 3920414, 9 pages, 2019.

[33] N. Niroshan, L. Yin, N. Sivakugan, and R. L. Veenstra, "Relevance of sem to long-term mechanical properties of cemented paste backfill," *Geotechnical and Geological Engineering*, vol. 36, no. 4, pp. 2171–2187, 2018.

[34] A. N. Pan, M. W. Grabinsky, and L. Guo, "Shear properties of cemented paste backfill under low confining stress," *Advances in Civil Engineering*, vol. 2021, Article ID 561977, 11 pages, 2021.

[35] S. Ning, W. Zhu, X. Yi, and L. Wang, "Evolution law of floor fracture zone above a confined aquifer using backfill replacement mining technology," *Geofluids*, vol. 2021, Article ID 8842021, 14 pages, 2021.

[36] K. Polak, K. Różkowski, and P. Czaja, "Causes and effects of uncontrolled water inrush into a decommissioned mine shaft," *Mine Water and the Environment*, vol. 35, no. 2, pp. 128–135, 2016.

[37] M. Sheshpari, "A review of underground mine backfilling methods with emphasis on cemented paste backfill," *Electronic Journal of Geotechnical Engineering*, vol. 20, no. 13, pp. 5183–5208, 2015.

[38] Y. Sun, G. Li, N. Zhang, Q. Chang, J. Xu, and J. Zhang, "Development of ensemble learning models to evaluate the strength of coal-grout materials," *International Journal of Mining Science and Technology*, vol. 31, no. 2, pp. 153–162, 2021.